Supporting Information

Self-Sealing Carbon Patterns by One-Step Direct Laser Writing and Their Use in Multifunctional Wearable Sensors

*Yanbo Yao, Zhufeng Jiang, Jingwen Yao, Jiangjiang Luo, Chang Xu, Jinyu Chong, Tao Liu**

College of Chemistry, Chemical Engineering and Materials Science, Soochow University, Soochow, 215123, P. R. China

E-mail: tliu@suda.edu.cn

S1. Commercial Si strain gauge as a benchmark to validate the cantilever testing method in piezoresistive performance evaluation

By following the similar test procedures used in our previous work,[1,2] a cantilever made of stainless steel (length × width ×thickness = 40 mm×12 mm×0.3 mm) was used to test the piezoresistive performance of a commercial Si strain gauge in both tension and compression mode. The resultant resistance change of the Si strain gauge at different strain levels in both tension and compression is shown in **Figure S1,** in which the averaged strain experienced by the strain gauge was determined by the free-end deflection amplitude of the cantilever according to Eq. (2) in Ref. [2]. The experimentally determined GF was obtained by linear fitting the fractional relative resistance change $-[R(\varepsilon_{avg}) - R(0)]/R(0)$ versus the averaged strain ε_{avg}. The result is 115, which agrees with the manufacturer reported value 110.

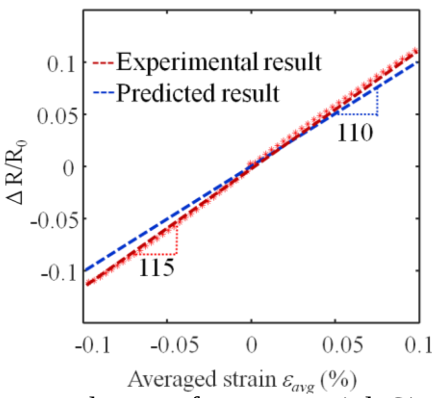

Figure S1. Relative resistance change of a commercial Si strain gauge under tension and compression evaluated by a cantilever testing method.

S2. Photothermal modeling and simulation for IR-DLWc

By using the similar COMSOL® photothermal model established in our previous work for the conventional DLWc process of PI film,[3] we carried out FEA modeling for the IR-DLWc process. The modification made in the present model is to explicitly consider the conductive heat transfer effect of the superstrate (ZnSe) and the substrate (aluminum, Invar alloy or fused quartz). Moreover, in order to account for the reflection loss of the laser beam at the interface of ZnSe/PI and Air/ZnSe, the corresponding reflection coefficients at these two interfaces were estimated according to the refractive indices of the involved medium (ZnSe – 2.403; PI – 1.75+0.03i). The values are 0.025 and 0.17, respectively. For simplicity, in the FEA simulation, the density, thermal conductivity, and heat capacity for all components were considered temperature independent; and the values are listed in **Table S1**. All boundary conditions were set in natural convection with the ambient environment at room temperature. **Figure S2**a, S2b, and S2c respectively shows the temperature distribution of the PI film when the three layer structure of ZnSe/PI/Fused Quartz, ZnSe/PI/Aluminum, and ZnSe/PI/Invaralloy is irradiated by the CO_2 laser beam at 2 W for 15 msec. With 858K as the pyrolysis/carbonization temperature of PI (white contour lines highlighted in Figure S2), the residual PI thicknesses at the sides of superstrate and substrate are also indicated in the same figure.

Table S1. Density, thermal conductivity and heat capacity used in the FEA simulation for the photothermal carbonization of a superstrate/PI/substrate three-layer structure

		Density (m^3/kg)	Thermal conductivity (W/m/K)	Heat capacity (J/kg/K)
Superstrate (2 mm thick)	ZnSe	5720	18.2	343
PI film (50 μm thick)		1420	0.224	1060
Substrate (1 mm thick)	Aluminum	2700	222	940
	Fused quartz	2200	1.4	730
	Invar alloy	8150	13.5	515

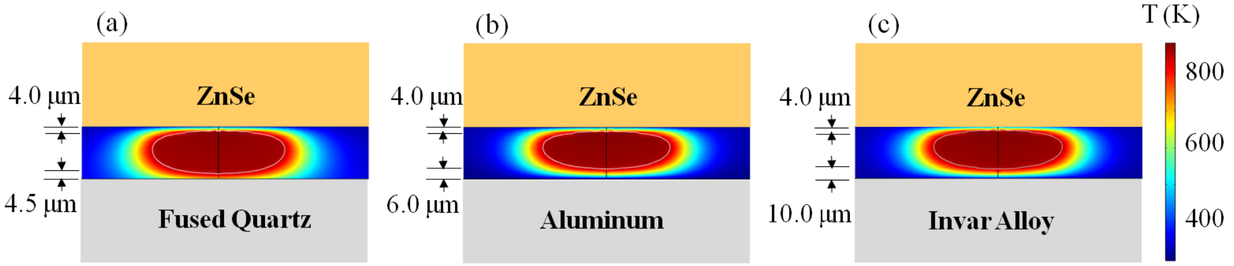

Figure S2. FEA simulated temperature distribution of the PI film in (a) ZnSe/PI/Fused Quartz; (b) ZnSe/PI/Aluminum; and (c) ZnSe/PI/Invar when being irradiated by CO_2 laser beam at 2 W for 15 msec. The highlighted white contour line indicates the temperature of 858K, at which the pyrolysis/carbonization of PI occurs.

S3. Strain-engineering treatment of the self-sealed carbon line for enhancing its piezoresistive sensitivity

A strain-engineering treatment was adopted to enhance the piezoresistive sensitivity of the as-prepared self-sealed carbon line fabricated by IR-DLWc. The treatment was performed by manually folding and sliding the PI film embedded with the sealed carbon line around a steel bar of 0.4 mm in diameter, as schematically shown in **Figure S3**. Considering the asymmetric nature of the sealing in the thickness direction of the carbon line fabricated by IR-DLWc, the folding and sliding have been performed in two different ways: one is to fold the PI film toward the side in contact with Invar alloy (substrate) (**Figure S3**– Type A) and another is to fold it toward the side in contact with ZnSe (superstrate) (**Figure S3**– Type B). The carbon lines treated in these two different ways manifested qualitatively different resistance change behavior. In the former case (Type A), the resistance of the carbon line increased with increasing its curvature during folding and sliding treatment. However, in the latter situation (Type B), its resistance decreased while the curvature of the carbon line was increasing. Moreover, the absolute value of the maximum relative resistance change observed in Type A treatment was significantly higher than that in Type B treatment, which suggests that the Type A treatment could be an effective way for increasing the piezoresistive sensitivity of the self-sealed carbon line fabricated by IR-DLWc.

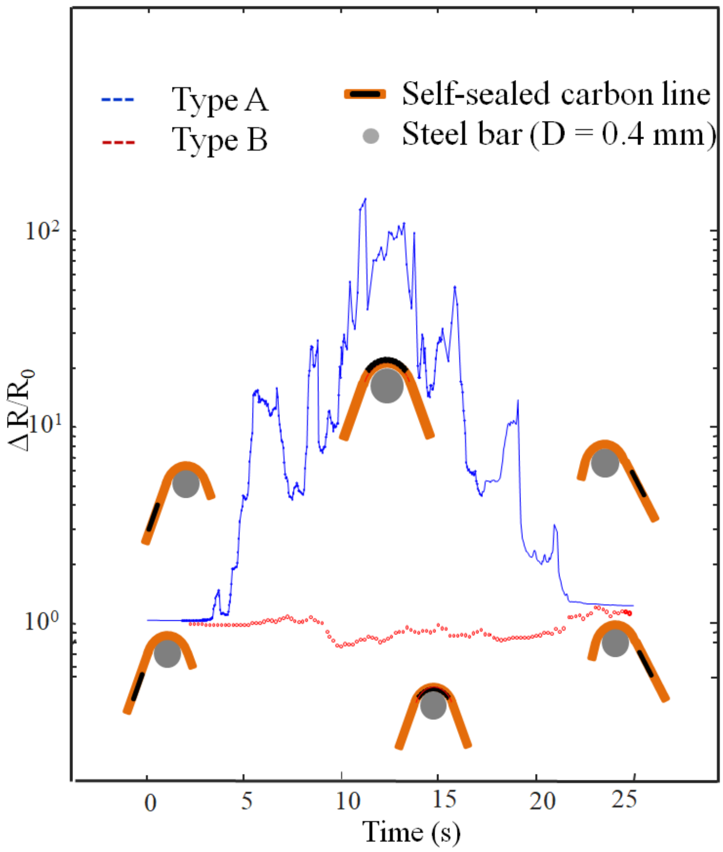

Figure S3. Schematic diagrams of the two different ways for performing the strain engineering treatments to the PI thin film embedded with a self-sealed carbon line and the corresponding resistance change recorded in real-time. Type A: the side of the PI film in contact with Invar alloy facing towards the cylindrical steel bar; Type B: the side of the PI film in contract with ZnSe window facing towards the cylindrical steel bar.

S4. Effect of double writing on the morphology and structure of the IR-DLWc created carbon line feature

Figure S4a and S4b respectively show the optical and SEM micrographs of a self-sealed carbon line created by IR-DLWc with double writing scheme (P = 2 W; scanning speed = 15 mm/sec). Upon double writing, the self-sealing character of the carbon line was not destroyed. As compared to the single-writing carbon line, the double writing seems resulted a more porous structure, though the degrees of order of the carbonaceous structure has not been improved much as shown by the Raman spectra shown in Figure S4c.

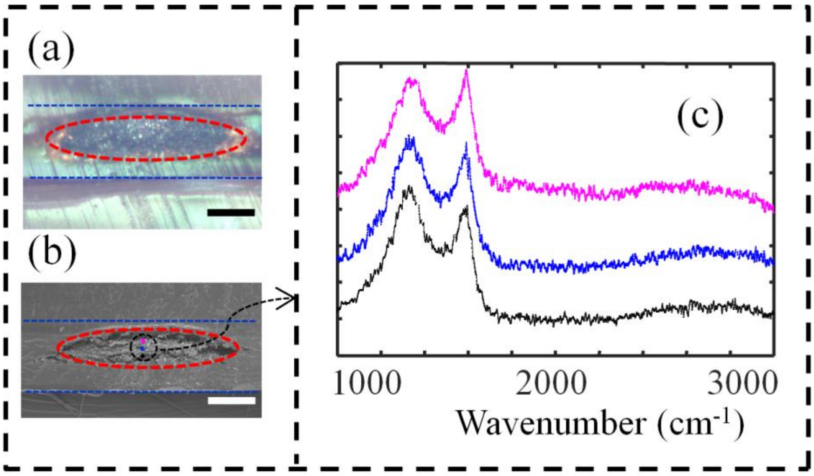

Figure S4. Optical and SEM micrographs of the cross-section view (a, b) and its Raman spectra (c) of a self-sealed carbon line created by IR-DLWc with a double writing scheme (P = 2 W; scanning speed = 15 mm/sec). In (a) and (b), the red-colored and blue-colored dash curves are respectively used to delineate the carbonization region and the surface boundary of the intact PI film. The scale bar is 50 μm.

S5. Establishment of the joint bending angle with respect to the resistance change of the self-sealed carbon line

With the same methods to obtain the quantitative correlation between the bending angle of the proximal interphalangeal joint of the index finger with the relative resistance change of the corresponding carbon line sample (Figure 6d), we established the similar correlations for all the 14 carbon lines located at the different joints in the glove sensor (Figure 6a). The results are shown in **Figure S5**.

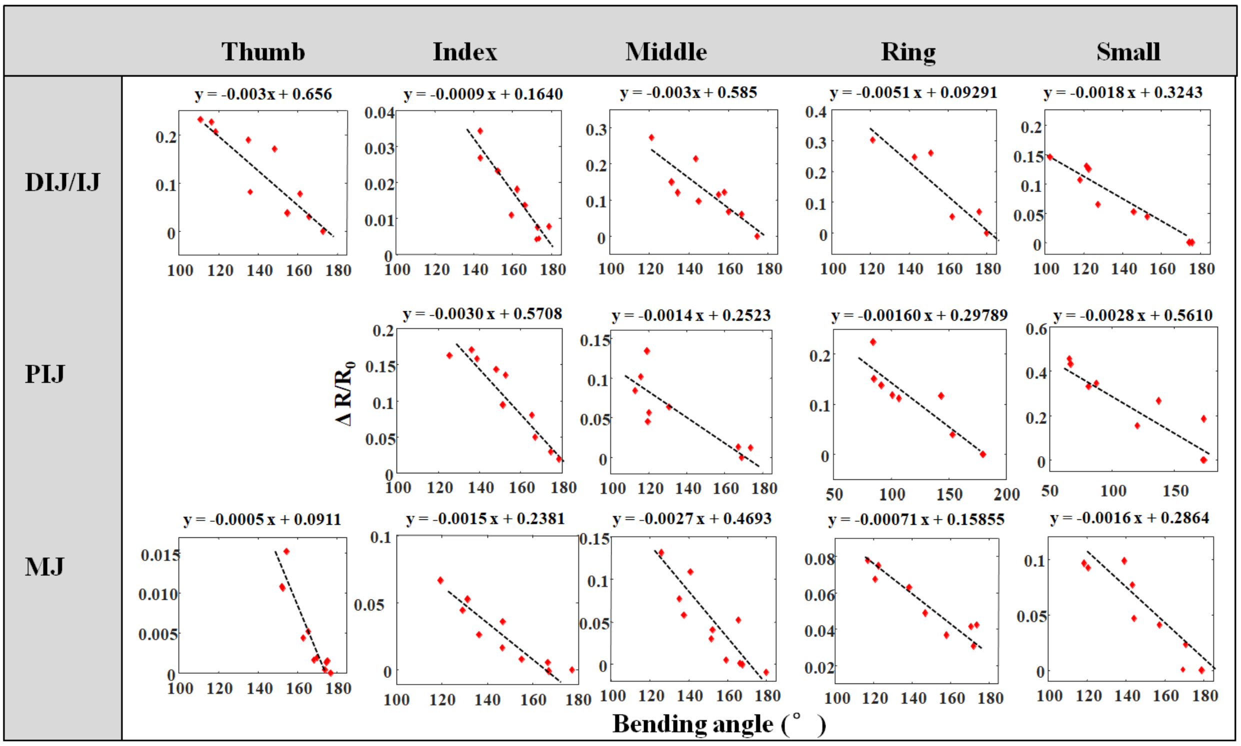

Figure S5. Quantitative correlation between the relative resistance of the carbon line and the bending angle of its associated joint.

Reference

(1) Luo, J.; Yao, Y.; Duan, X.; Liu, T. Force and Humidity Dual Sensors Fabricated by Laser Writing on Polyimide/Paper Bilayer Structure for Pulse and Respiration Monitoring. *J. Mater. Chem. C* **2018**, *6*, 4727-4736.

(2)Yao, Y.; Luo, J.; Duan, X.; Liu, T.; Zhang, Y.; Liu, B. M., Yu, M. On the piezoresistive behavior of carbon fibers - Cantilever-based testing method and Maxwell-Garnett effective medium theory modeling *Carbon* **2019**, *141*, 283-290.

(3) Ruan, X.; Wang, R.; Luo, J.; Yao, Y.; Liu, T. Experimental and Modeling Study of CO_2 Laser Writing Induced Polyimide Carbonization Process. *Mater. Design* **2018**, *160*, 1168-1177.